



HAL
open science

Synthesis of goethite from Fe(OH) precipitates: Influence of Fe(II) concentration and stirring speed

F. Françoise Gilbert, Philippe Refait, F. François Lévêque, C. Céline
Remazeilles, Egle Conforto

► To cite this version:

F. Françoise Gilbert, Philippe Refait, F. François Lévêque, C. Céline Remazeilles, Egle Conforto.
Synthesis of goethite from Fe(OH) precipitates: Influence of Fe(II) concentration and stirring speed.
Journal of Physics and Chemistry of Solids, 2009, 69 (8), pp.2124. 10.1016/j.jpcs.2008.03.010 . hal-00547307

HAL Id: hal-00547307

<https://hal.science/hal-00547307>

Submitted on 16 Dec 2010

HAL is a multi-disciplinary open access archive for the deposit and dissemination of scientific research documents, whether they are published or not. The documents may come from teaching and research institutions in France or abroad, or from public or private research centers.

L'archive ouverte pluridisciplinaire **HAL**, est destinée au dépôt et à la diffusion de documents scientifiques de niveau recherche, publiés ou non, émanant des établissements d'enseignement et de recherche français ou étrangers, des laboratoires publics ou privés.

Author's Accepted Manuscript

Synthesis of goethite from $\text{Fe}(\text{OH})_2$ precipitates:
Influence of $\text{Fe}(\text{II})$ concentration and stirring speed

Françoise Gilbert, Philippe Refait, François Lévêque,
Céline Remazeilles, Egle Conforto

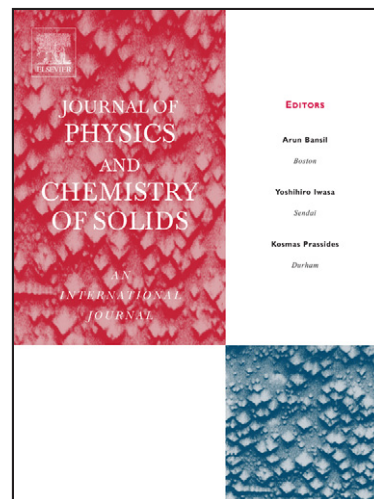
PII: S0022-3697(08)00071-1
DOI: doi:10.1016/j.jpccs.2008.03.010
Reference: PCS 5410

To appear in: *Journal of Physics and
Chemistry of Solids*

Received date: 5 July 2007
Revised date: 7 February 2008
Accepted date: 11 March 2008

Cite this article as: Françoise Gilbert, Philippe Refait, François Lévêque, Céline Remazeilles and Egle Conforto, Synthesis of goethite from $\text{Fe}(\text{OH})_2$ precipitates: Influence of $\text{Fe}(\text{II})$ concentration and stirring speed, *Journal of Physics and Chemistry of Solids* (2008), doi:10.1016/j.jpccs.2008.03.010

This is a PDF file of an unedited manuscript that has been accepted for publication. As a service to our customers we are providing this early version of the manuscript. The manuscript will undergo copyediting, typesetting, and review of the resulting galley proof before it is published in its final citable form. Please note that during the production process errors may be discovered which could affect the content, and all legal disclaimers that apply to the journal pertain.



www.elsevier.com/locate/jpcs

Synthesis of goethite from Fe(OH)₂ precipitates: influence of Fe(II) concentration and stirring speed

Françoise Gilbert^a, Philippe Refait^{b*}, François Lévêque^a, Céline Remazeilles^b, Egle Conforto^c

^a *Littoral Environnement et Sociétés, UMR 6250, CNRS-Université de La Rochelle, 2 rue*

Olympe de Gouges, F-17000 La Rochelle, France

^b *Laboratoire d'Etude des Matériaux en Milieu Agressif, EA3167, Université de La Rochelle,*

Bâtiment Marie Curie, Avenue Michel Crépeau, F-17042 La Rochelle cedex 01, France

^c *Centre Commun d'Analyse, Université de La Rochelle, 5 Perspective de l'Océan, F-17071*

La Rochelle cedex 09, France

Abstract. Magnetic methods are efficient tools in soil and environmental science. But in such natural environments, several magnetic carriers are generally present. So, synthetic standard samples are necessary for calibration of laboratory techniques. The aim of this study was to synthesize goethite free of magnetic impurities (concentration $< \sim 1 \mu\text{g kg}^{-1}$) with different crystal sizes. Goethite was prepared by oxidation of aqueous suspensions of Fe(OH)₂ precipitates. Final products were characterized by X-ray diffraction, infrared spectroscopy, scanning and transmission electron microscopy and magnetic methods. Goethite could be obtained in the absence of any trace of strong magnetic carriers using FeSO₄ • 7H₂O and NaOH as reactants with the following experimental conditions: temperature = 45 °C, [FeSO₄ • 7H₂O] = 0.50 mol L⁻¹, [NaOH] = 0.20 mol L⁻¹, stirring speed = 760 rpm. The Fe(II) concentration and the stirring speed were varied. It proved possible to modify the size of the goethite crystals by varying the Fe(II) concentration and the stirring speed, but important changes of these parameters induced the formation of other phases, lepidocrocite when the oxidation reaction was drastically accelerated and Fe₃O₄ when the reaction was slowed down.

In any case, for weak magnetic fields, a low coercivity saturation step was observed. It may be attributed to traces of δ -FeOOH or to domains structurally similar to δ -FeOOH inside the multidomainic crystals of α -FeOOH.

Keywords: A. Magnetic materials. B. Chemical synthesis. B. Crystal growth. D. Crystal structure. D. Magnetic properties.

* Corresponding author. Tel. : (33)5 46 45 82 27

Fax : (33)5 46 45 72 72

E-mail address : prefait@univ-lr.fr

1. Introduction

In natural environments such as soils, iron oxides (i.e. oxides, hydroxides, oxyhydroxides) are generally present in small quantity (which could be lower than g kg^{-1}), even though their presence and distribution depend on the availability of iron and on environmental conditions [1,2]. This weak concentration, the small crystal size and the low crystallinity make difficult the study of these compounds by spectroscopic methods and diffraction techniques. In some cases information can be obtained by use of selective methods only sensitive to iron, e.g. ^{57}Fe Mössbauer spectroscopy or X-ray absorption spectroscopy at the Fe-K edge. Some iron oxides can also be studied with high resolution thanks to their magnetic properties, with semi-quantification for concentrations in the order of mg kg^{-1} [3]. The magnetic parameters measured are related to the capacities of magnetisation, their dependence to field intensity induced and temperature. Remanent magnetisation is for instance a parameter commonly studied. The magnetic properties depend on nature, concentration, and crystal size of magnetic carriers. Pure samples with controlled crystal size are then necessary for calibration of protocols.

Magnetite and Fe(III) oxyhydroxides can be prepared by oxidation of aqueous suspensions of Fe(II) precipitates. The initial Fe(II) precipitate is obtained by mixing a solution of NaOH with a solution of a Fe(II) salt, typically $\text{FeSO}_4 \cdot 7\text{H}_2\text{O}$ or $\text{FeCl}_2 \cdot 4\text{H}_2\text{O}$. A magnetic stirrer insures the homogeneity of the oxidation process. The nature of the final products of the oxidation depends on various parameters such as concentration of the reactants, concentration ratio $[\text{Fe}^{2+}] / [\text{OH}^-]$, temperature, stirring speed and nature of the Fe(II) salt [4-17]. These parameters also influence the size and morphology of the crystals, and the crystallinity of the final product [15-17]. Note that under natural conditions, various species such as phosphates or silicates can hinder crystal growth and heavily influence reaction pathways.

Goethite ($\alpha\text{-FeOOH}$) is one of the magnetic carriers commonly found in natural environments (soils, sediments, etc...). As a matter of fact, the oxidation of Fe(II) will be the preferred natural pathway for its formation. Goethite is characterised by a weak capacity to carry remanent magnetisation (it is imperfect antiferromagnetic at room temperature), and the saturation is reached for magnetic fields beyond the instrumental means usually available [18]. A study of the magnetic properties of goethite implies the absence of any traces of other magnetic phases such as magnetite, maghemite or hematite that have a strong magnetic signal with weak magnetic fields.

This study was then devoted to the synthesis of goethite by oxidation of aqueous suspensions of Fe(II) precipitates. The first objective was to specify the experimental conditions adequate to prepare goethite without strong magnetic carriers, or more exactly so that other magnetic phases can not be detected by magnetic measurements. The second objective was to clarify the influence of various parameters, namely stirring speed and concentration of reactants, on the formation of goethite and on its crystal size.

2. Experimental

2.1. Synthesis of goethite without strong magnetic carriers

Numerous studies were devoted to the oxidation of Fe(II) compounds precipitated by mixing sodium hydroxide and Fe(II) salt solutions. The experimental conditions favouring goethite formation are then already known. First, chloride ions favour lepidocrocite [8,13], and $\text{FeSO}_4 \cdot 7\text{H}_2\text{O}$ has to be preferred to $\text{FeCl}_2 \cdot 4\text{H}_2\text{O}$ as the initial Fe(II) salt. Secondly, the parameter playing the major role is $R = [\text{Fe}^{2+}]/[\text{OH}^-] = [\text{FeSO}_4]/[\text{NaOH}]$, the concentration ratio of the reactants [6,9,10,12]. Goethite forms preferentially with a large excess of OH^- ions, e.g. $R = 0.2$, or with a large excess of Fe^{2+} ions, e.g. $R = 2.5$ [6,9,10,12,15], with respect to the stoichiometric conditions of the precipitation of $\text{Fe}(\text{OH})_2$, that is $R = 0.5$ according to the reaction:



As the kinetics of the reaction is controlled by the reduction of dissolved O_2 , temperature is another important parameter since it modifies the solubility of oxygen. For the largest temperatures (low solubility of oxygen), typically $T \geq 60 \text{ }^\circ\text{C}$, Fe_3O_4 forms preferentially [7,8,10]. For the lowest temperatures (larger solubility of oxygen), $T \leq 20 \text{ }^\circ\text{C}$, lepidocrocite $\gamma\text{-FeOOH}$ is favoured [8,9,11]. This explains why goethite is often obtained at intermediate temperatures, between 25 and 45 $^\circ\text{C}$ [8,9,11,12,15].

Two experimental conditions were then retained as reference conditions appropriate for goethite formation. In each case, 200 mL of suspension were prepared by mixing 100 mL of a $\text{FeSO}_4 \cdot 7\text{H}_2\text{O}$ solution with 100 mL of a NaOH solution. The rotation speed of the magnetic stirrer was set at 760 rpm. The first experimental reference is defined by the following conditions:

$T = 25 \text{ }^\circ\text{C}$, $[\text{FeSO}_4 \cdot 7\text{H}_2\text{O}] = 0.15 \text{ mol L}^{-1}$, and $R = 0.2$ (then $[\text{NaOH}] = 0.75 \text{ mol L}^{-1}$).

The second experimental reference corresponds to:

$T = 45\text{ }^{\circ}\text{C}$, $[\text{FeSO}_4 \cdot 7\text{H}_2\text{O}] = 0.50\text{ mol L}^{-1}$, and $R = 2.5$ (then $[\text{NaOH}] = 0.20\text{ mol L}^{-1}$).

Note that the mechanisms of formation of goethite are different [10]. With experimental conditions (I), goethite forms directly from $\text{Fe}(\text{OH})_2$. With experimental conditions (II), goethite forms from an intermediate $\text{Fe}(\text{II-III})$ compound, the $\text{Fe}(\text{II-III})$ hydroxysulphate green rust.

The chemicals, provided by Aldrich®, ensured a 98% min. purity. X-ray diffraction (XRD) analyses and magnetic measurements were performed on the $\text{Fe}(\text{II})$ sulphate. XRD demonstrated that it was mainly made of melanterite ($\text{FeSO}_4 \cdot 7\text{H}_2\text{O}$) with traces of rozenite ($\text{FeSO}_4 \cdot 4\text{H}_2\text{O}$). The impurities did not give any magnetic signal. The 200 mL suspension was aerated at the liquid-air interface in a beaker of 9-cm diameter. The magnetic stirring ensured a progressive homogeneous oxidation of the precipitate. The temperature was controlled by a thermostat with accuracy of $\pm 0.5^{\circ}\text{C}$. All experiments were carried out at 25 or 45°C . Further details about this methodology can be found in previous works [6-17].

Once the experimental conditions leading to goethite were clearly defined, it was envisioned to modify the size of the crystals by varying the stirring speed and the $\text{FeSO}_4 \cdot 7\text{H}_2\text{O}$ concentration. As the nature of the final product of oxidation is mainly sensitive to the concentration ratio R and the temperature T [6,8-12,15], those parameters were kept at the values corresponding to the experimental conditions leading to goethite without strong magnetic carriers.

The crystal size is likely to be modified by a change in the kinetics of goethite formation. The reaction is controlled by the kinetics of the reduction of dissolved O_2 . A decrease of the $\text{Fe}(\text{II})$ concentration decreases the $[\text{Fe}(\text{II})]/[\text{O}_2]$ ratio, so increases the oxidation rate and decreases the crystal size. Similarly, an increase of the stirring speed induces an increase of the area of the air/suspension interface, and consequently an increase of

the oxygen flow, which would lead to a decrease of the crystal size. Stirring speeds from 430 to 1200 rpm were then tested whereas $[\text{FeSO}_4 \cdot 7\text{H}_2\text{O}]$ was varied from 0.1 to 1.0 mol L⁻¹.

2.2. Goethite characterisation and crystal size analysis

Final products were characterised by powder X-ray diffraction (PXRD), diffuse reflectance infrared Fourier transform spectroscopy (DRIFTS), scanning and transmission electron microscopy (SEM and TEM) and magnetic methods. The powders were obtained after centrifugation of the precipitates, drying and crushing. Each sample was rinsed thoroughly so as to remove the soluble salt (Na_2SO_4) that forms during drying.

PXRD analyses were performed on a Bruker AXS® D8-Advance diffractometer in Bragg-Brentano geometry using $\text{CuK}\alpha$ radiation ($\lambda = 0.15406$ nm). The acquisition time was 5 seconds with 2θ varying from 10 to 60° by steps of 0.04°. No internal standard was added for peak position calibration. The mean coherence lengths were estimated from XRD line broadening using the Scherrer formula:

$$D_{\text{hkl}} = 0.9 \lambda / w \cdot \cos\theta_{\text{hkl}} \quad (2)$$

where D_{hkl} is the mean coherence length of the particles in the direction perpendicular to the (hkl) planes, λ the wavelength of the X-rays, w the full width at half maximum of the hkl diffraction line at $2\theta_{\text{hkl}}$. The width at half maximum w was corrected from the instrumental line broadening ($\sim 0.04^\circ$ at $2\theta_{\text{hkl}} \sim 20^\circ$) determined from the XRD analysis of a standard quartz sample.

DRIFTS measurements were performed at ambient temperature on a Thermo Nicolet FT-IR Nexus spectrometer using a KBr beamsplitter, a DTGS detector and a Smart Diffuse Reflectance accessory. The spectra were recorded with the Omnic software at a resolution of 4 cm⁻¹, with 64 scans and a gain of 1. The powder to be analysed was diluted in KBr (95%

KBr, 5% FeOOH). The background spectrum was acquired with a mirror-polished stainless steel standard sample before the analysis of each oxidation product.

Morphology and size of the particles were analyzed by SEM (Quanta 200 ESEM/FEG, Philips). Observations were carried out at 20 kV, under 0.75 mbar of water vapour pressure (Low-Vacuum mode), using a Large-Field Gaseous detector for secondary electron-type images. Samples were dispersed in ethanol using sodium hexametaphosphate as dispersing agent [19] and an ultrasonic stirring. A drop of the solution was placed on a polished carbon SEM mount. Once dried, a very fine layer of carbon was deposited above the sample. The sample obtained with $R = 2.5$, $[\text{FeSO}_4] = 0.50 \text{ mol L}^{-1}$, $T = 45^\circ\text{C}$ and $S = 760 \text{ rpm}$ was also characterised by transmission electron microscopy (TEM) with a JEOL JEM 2011 (200 kV) apparatus. Here, a drop of the solution was directly placed on a copper grid covered with a carbon film.

In environmental magnetism, the parameters used for characterisation [19,20] depend on magnetic behaviour. The results presented in this article are the backfield (BF) of Isothermal Remanent Magnetisation (IRM) acquisition curves. The method consists in reversing the IRM by gradually increasing the applied magnetic field. The steps of the magnetisation curve are attributed to changes of mineralogy. The magnetisation is proportional to the amount of the corresponding magnetic carrier. Let us consider magnetite as an example. The concentration would be estimated by dividing the value of the IRM saturation (in $\text{A m}^2 \text{ kg}^{-1}$) of the sample by the remanent saturation magnetisation (σ_{rs}) of magnetite. The main error is due to the variability of the value of σ_{rs} , comprised between 3.6 and $10.2 \text{ A m}^2 \text{ kg}^{-1}$ for magnetite [21]. Since each magnetic mineral contributes to the BF IRM, its interpretation may be difficult when several magnetic carriers are present in the sample. In this case, magnetic mineralogical composition can be studied via thermal

demagnetisation of multi-component IRM by identifying unblocking temperatures T_b [3,22]. For instance T_b is ~60-120°C for goethite and ~575°C for magnetite [22].

For magnetic measurements, samples (2 cm³) were consolidated using kaolin treated with acids and SiO₂ powder obtained by sol-gel process [23]. IRM was induced, until $B = 9$ T, by use of a Magnetic-Measurements MMPM 10 pulse magnetizer and measured with an Agico JR6 spinner magnetometer. The limit of detection of magnetite was estimated at about 1.5 µg kg⁻¹. BF IRM curves were plotted so as to facilitate the comparison with IRM curves. So, BF IRM = 0 corresponds to the saturation of forward IRM, and the change of the magnetisation with the increasing oppositely directed magnetic field is expressed as an increase of BF IRM (in A m² kg⁻¹). So the maximum value reached by BF IRM is the double of the saturation of forward IRM. This rescaling was done so as to keep the amplitude of the variations of magnetisation while the comparison between the curves of various samples was facilitated.

For thermal demagnetisation, IRM on three orthogonal axes were successively acquired in three decreasing magnetic fields: 9 T, 3 T and 0.5 T. Thermal demagnetisation was carried out with a Magnetic-Measurements MMTD 18 thermal demagnetiser. The sample was heated, cooled back to room temperature in zero magnetic field and the remanence was then measured. This operation was repeated with increasing temperature, up to total demagnetisation (< 1%). Temperature steps were 20°C, in the range considered here (60-140°C).

3. Experimental results

3.1. Synthesis of goethite without strong magnetic carriers: influence of stirring speed and FeSO₄ concentration

First, goethite was prepared according to the experimental conditions of reference

derived from previous works. In each case only goethite could be detected with the PXRD and DRIFTS analyses; results for conditions (II) are presented hereafter. Magnetic measurements were then performed. Figure 1 presents the BF-IRM curves obtained for each sample. They are clearly different. With the sample prepared in conditions (I), the magnetisation increased rapidly with a step of saturation. This behaviour is characteristic of a ferrimagnetic phase. It is more likely magnetite, as maghemite does not form in these conditions [10], and its approximate concentration would then be $1 \pm 1 \text{ g kg}^{-1}$. This illustrates the sensitivity of magnetic methods with respect to the detection of magnetic iron oxides. In contrast, the curve obtained with the sample prepared in conditions (II) is typical of an imperfect antiferromagnetic compound such as goethite. Consequently, experiment (II) was chosen as the unique reference for the rest of the study.

Fe(II) concentration and stirring speed were varied from the values corresponding to experience (II) ($[\text{FeSO}_4] = 0.5 \text{ mol L}^{-1}$ and $S = 760 \text{ rpm}$). First, it was verified that the decrease of $[\text{FeSO}_4]$ and the increase of S accelerated significantly the oxidation process. The duration t_F of the overall reaction was determined as explained elsewhere [12,15]. For experiment (II), $t_F = 18 \text{ h}$. It decreased down to 4 h for $S = 1200 \text{ rpm}$ and increased up to 40 h for $S = 430 \text{ rpm}$. Similarly, it decreased down to 3 h for $[\text{FeSO}_4] = 0.1 \text{ mol L}^{-1}$ and increased up to 27 h for $[\text{FeSO}_4] = 1.0 \text{ mol L}^{-1}$.

XRD (Fig. 2) shows that goethite was the main product obtained in all cases. However, the main diffraction line of lepidocrocite $\gamma\text{-FeOOH}$ is visible for the smaller Fe(II) concentrations, 0.1 and 0.125 mol L^{-1} . Moreover, important line broadenings are observed for the largest stirring speed, 1200 rpm, and the smaller Fe(II) concentration, 0.1 mol L^{-1} . An increase of the stirring speed and a decrease of the Fe(II) concentration correspond to an increase of the oxidation rate. Since a line broadening corresponds to a decrease of the coherence length in the goethite particles, these results confirm that a change of the kinetics

modifies the crystallinity and/or the crystal size. Note also that the small signal-to-noise ratio of the pattern of goethite obtained with the smaller Fe(II) concentration is also more likely due to the decrease of crystallinity and/or crystal size.

The infrared spectra were acquired from 400 to 4000 cm^{-1} but the main changes occurred between 400 and 1400 cm^{-1} . Fig. 3 is then focused on this wavenumber interval. The main vibration bands generally attributed to goethite [24] are found in any case at 630, 795 and 890 cm^{-1} . The main vibration bands of lepidocrocite, at 610, 750, 1020 and 1150 cm^{-1} [25] are visible for 0.1 and 0.125 mol L^{-1} , in agreement with XRD analysis. However, a small band at 1020 cm^{-1} is seen at $S = 1200$ rpm, indicating that lepidocrocite was also obtained with the largest stirring speed. Additional bands at 975, 1055 and 1130 cm^{-1} may be attributed to sulphate ions adsorbed on the surface of the goethite crystals [26].

Magnetic characterisation was performed to study the magnetic properties of goethite and to determine if other magnetic phases had formed (Fig. 4). Lepidocrocite is paramagnetic at ambient temperature and cannot be detected by magnetic measurements. Fig. 4a shows that magnetisation rapidly increases with a step of saturation at about 0.2 T for the lower stirring speeds, $S = 510$ and 430 rpm. This demonstrates that a small amount of magnetite has formed for the slower oxidation kinetics. The amount of magnetite can be estimated at 0.2 ± 0.2 mg kg^{-1} for 510 rpm and 0.3 ± 0.3 mg kg^{-1} for 430 rpm from the BF IRM values at saturation. For samples free of magnetite, modifications of stirring speed (Fig. 4a) and Fe(II) concentration (Fig. 4b) also induced changes in magnetic properties. These changes may be due to changes of crystal size and/or crystallinity of the goethite particles. Finally, for weak magnetic fields, a low coercivity saturation step is observed (Figs. 4c,d). It looks like the behaviour of magnetite. But the contribution of this low coercivity phase increases when S increases and when $[\text{FeSO}_4]$ decreases, that is when the kinetics of the reaction increases. An increase of the kinetics favours lepidocrocite, not magnetite [6,16]. So this phenomenon is not related to

magnetite formation. Additional magnetic experiments were performed so as to determine its origin. They are described in section 3.3.

3.2. Crystal size analysis

Morphology and size of the particles were analysed from images obtained with SEM. A sample of goethite prepared in the experimental conditions of reference (II) was first observed with TEM. Both SEM and TEM observations were in agreement, showing needle-like crystals of goethite with an average length of $0.7 \pm 0.2 \mu\text{m}$ and an average width of $0.08 \pm 0.02 \mu\text{m}$. The particles were also observed using backscattered electron imaging without carbon deposit (compositional contrast) and crystal sizes were the same as those observed by secondary electron-type imaging. Fig. 5 shows examples of the images obtained. Fig. 5a is a typical TEM photograph of the acicular crystals of goethite obtained in the experimental conditions of reference (II). The detailed exploration of this sample however revealed the presence of a few crystals with a totally different morphology (Fig. 5b). They resemble somewhat to the crystals of a hexagonal phase generally associated to goethite, called α' -FeOOH by Olowe et al. [15] but similar to δ -FeOOH. However, electron diffraction patterns obtained with those crystals were not sharp enough (crystals show a low degree of crystalline order) to allow an unambiguous identification of the phase. Figs 5c and d are SEM photographs of the goethite crystals obtained at $[\text{FeSO}_4] = 1.0 \text{ mol L}^{-1}$ and 0.1 mol L^{-1} , respectively. They clearly illustrate that the morphology of particles does not change and that their size decreases with the Fe(II) concentration.

The determination of the crystal size was carried out for each sample from about a hundred particles via SEM photographs. Variation of the stirring speed proved to have influence on the size of the particles. Their average length varies from $0.6 \pm 0.2 \mu\text{m}$ (1200 rpm) to $0.8 \pm 0.1 \mu\text{m}$ (430 rpm). The effect of the variation of the Fe(II) concentration

modifies more strongly the crystal size. The average length varies from $0.5 \pm 0.1 \mu\text{m}$ (0.1 mol L^{-1}) to $1.1 \pm 0.3 \mu\text{m}$ (1.0 mol L^{-1}).

Synthetic goethite crystals are acicular, with a large crystal length to crystal width ratio, as seen in Fig. 5. According to previous works [1], they are elongated along the [001] direction (c -axis of the orthorhombic structure with Pbnm space group). Goethite crystals are generally constituted of various domains (also called crystallites or intergrowths) [1,27,28]. The domains frequently extend along the c -axis and are stacked along the a - and b - axes. The mean coherence lengths (MCLs), determined from XRD patterns using the Scherrer formula (2), are then smaller than the crystal size. D_{110} , associated with the most intense diffraction line, and D_{020} were estimated so as to illustrate the variations of MCLs with Fe(II) concentration and stirring speed. D_{110} remains almost constant at $19 \pm 3 \text{ nm}$ when $[\text{FeSO}_4]$ varies. In contrast, D_{020} decreases from 40 down to 10 nm when $[\text{FeSO}_4]$ decreases from 1.0 down to 0.1 mol L^{-1} . But D_{020} is significantly smaller only for 0.125 mol L^{-1} (19 nm) and 0.1 mol L^{-1} (10 nm) i.e. when lepidocrocite forms together with goethite. So, this rapid decrease of D_{020} is associated to the appearance of lepidocrocite as a component of the final product. The increase of the kinetics of the reaction favours the formation and growth of the lepidocrocite crystals and hinders the growth of the goethite crystals. The effects of the stirring speed are weaker. D_{110} slightly decreases from 26 to 14 nm as S increases from 430 to 1200 rpm. D_{020} is constant for S between 510 and 1200 rpm, with a value equal to $28 \pm 2 \text{ nm}$. It changes only for 430 rpm, where it reaches 40 nm.

The width and length obtained from SEM are higher than the MCLs estimated from XRD. This confirms that goethite crystals are constituted of various domains. MCLs reflect the size of these domains whereas SEM measurements reflect that of the crystals. The width (SEM) to D_{110} (XRD) ratio lies between 2.4 and 6.4. It is in most cases equal to 2.4-2.8 except for $[\text{FeSO}_4] = 0.1 \text{ mol L}^{-1}$. D_{110} is almost unaffected by the variations of the Fe(II)

concentration. So the ratio varied because the width measured by SEM varied whereas the MCL measured by XRD remained constant. The MCL that was observed to vary is D_{020} that was divided by a factor 4. D_{020} and the width measured by SEM behave similarly. It can be forwarded that this width corresponded in most cases to the elongation of the crystals along the [010] direction (b -axis).

3.3. Magnetic behaviour in weak magnetic field

The low coercivity behaviour of goethite could be associated whether to the presence of a ferrimagnetic carrier (e.g. magnetite) in very low concentration or to the presence of defects in the structure of goethite [29,30]. The results of thermal demagnetisation of goethite obtained using the experimental conditions of reference (II) are presented in Fig. 6. The decay of remanence intensity was measured after each thermal demagnetisation step. The little hump at 100°C on the curve for 0.5 T is more likely due to misorientation in the magnetometer. The main result is that demagnetisation occurred for an unblocking temperature of 120°C. This value is characteristic of goethite [22] which excludes the presence of magnetite. This is not a surprise as magnetite formation is favoured by the decrease of the stirring speed and the increase of the Fe(II) concentration while the low coercivity behaviour increases when these parameters vary in the opposite direction.

But it can be proposed that the low coercivity behaviour of goethite is related to traces of another magnetic compound, δ -FeOOH. This phase is generally considered as ferrimagnetic below $T_c \approx 170$ °C where the spins are parallel to $\langle 001 \rangle$ [31-32]. Moreover, the temperature of transformation of δ -FeOOH into goethite and hematite (120-150°C) [1,33-34] is close to the temperature of demagnetisation of goethite measured above.

4. Discussion

The traces of δ -FeOOH could correspond to the crystals observed on the TEM micrograph of Fig. 5b and/or to domains inside the goethite crystals that would have a structure close to that of δ -FeOOH. This assumption is based on the crystallography of α -FeOOH and δ -FeOOH. The pile up of anions is in each case hexagonal close packed (hcp). The only difference is the arrangement of the Fe^{3+} cations. In the case of α -FeOOH [e.g. 35], the cations occupy octahedral sites between two hexagonal planes of the anions in form of parallel bands in which two rows are completely occupied and two adjacent rows are empty. The occupancies are interchanged from plane to plane. The lattice is then orthorhombic, and the hexagonal arrangement of anions is distorted. The c -axis is parallel to the double bands of cations. In the case of δ -FeOOH, the cell is hexagonal and reflects the hcp stacking of anions [31-32,36-37]. The arrangement of the Fe^{3+} cations in the octahedral sites of the hcp stacking is then made at random or with an ordering compatible with the symmetry of a hexagonal or trigonal lattice. Olowe et al. [15] designated as “ α' -FeOOH” the completely disordered phase, considering α -FeOOH and δ -FeOOH as two different ordered forms.

This study by Olowe et al. [15] was devoted to the influence of Fe(II) concentration on goethite formation in experimental conditions close to the reference conditions (I) described above. In this case, the ratio R being equal to 0.2, there is an excess of NaOH with respect to the precipitation of $\text{Fe}(\text{OH})_2$ and goethite forms directly from $\text{Fe}(\text{OH})_2$. Lepidocrocite can not form. So, when the Fe(II) concentration became too small for goethite to form, another compound was obtained. Its XRD pattern was very similar to that of δ -FeOOH [15]. Olowe et al. [15] also observed progressive small changes on the XRD patterns of goethite. These changes indicated that the disordering of Fe^{3+} cations increased gradually as the Fe(II) concentration decreased, that is as the oxidation became faster.

It may be assumed that a similar disordering occurred in our experimental conditions when the oxidation was accelerated. The main difference is that in our conditions, where $R = 2.5$, $\text{Fe}(\text{OH})_2$ is oxidised first into the Fe(II-III) hydroxysulphate green rust [10], that is oxidised in turn into goethite. Then, goethite is obtained from the green rust. This explains why lepidocrocite, the main oxidation product of green rusts [10,12,13], has been obtained for the fastest reactions. The formation of lepidocrocite implies that the total disordering leading to the formation of $\delta\text{-FeOOH}$ instead of $\alpha\text{-FeOOH}$ can not be observed in our experimental conditions. But, due to the structural similarity between those compounds, it is probable that traces of $\delta\text{-FeOOH}$ have formed or that domains structurally similar to $\delta\text{-FeOOH}$ have grown inside the multidomainic goethite crystals, explaining the low coercivity behaviour observed in our samples.

5. Conclusion

The formation of goethite by oxidation of $\text{Fe}(\text{OH})_2$ precipitates in sulphated aqueous media is mainly controlled by the concentration ratio $R = [\text{Fe}^{2+}]/[\text{OH}^-] = [\text{FeSO}_4]/[\text{NaOH}]$ of the reactants, and by temperature T . It was then possible to determine adequate conditions for goethite formation, that is $R = 2.5$ and $T = 45^\circ\text{C}$, and synthetic samples free of magnetite could be obtained. These samples were analysed by magnetic methods the same way magnetic minerals in soils are usually studied.

To a lesser extent, Fe(II) concentration and stirring of the suspension also influence the nature of the final product, but mainly affect the kinetics of the reaction. Important variations of these parameters led to the formation of other phases, lepidocrocite when the reaction was accelerated, magnetite when it was slowed down. Determination of the magnetic properties of goethite samples confirmed that the formation of magnetite could be totally inhibited. Goethite crystals are generally made of the aggregation of similarly orientated

crystallites, as observed for goethite synthesised from ferrihydrite. Variations of concentration and stirring speed proved to induce significant variations of the size of the goethite crystals and crystallites.

For weak magnetic fields, a low coercivity saturation step was also detected. Its importance increased with increasing oxidation speed that is with increasing disorder in the arrangement of Fe^{3+} cations in the goethite structure. It is known that this disorder ultimately leads to the formation of $\delta\text{-FeOOH}$ [15], a ferrimagnetic compound. The low coercivity behaviour observed here may then correspond to traces of $\delta\text{-FeOOH}$ or to domains structurally similar to $\delta\text{-FeOOH}$ inside the multidomainic crystals of $\alpha\text{-FeOOH}$. The formation of $\delta\text{-FeOOH}$ crystals or $\delta\text{-FeOOH}$ -like domains inside goethite crystals is more likely inherent in goethite formation, due to the structural similarity between those phases.

Acknowledgements

The authors acknowledge the financial support by the Conseil General of Charente Maritime, France.

References

- [1] R. M. Cornell, U. Schwertmann, "The iron oxides: structure, properties, reactions and uses", Wiley-VCH, Weinheim, 2nd edition, 2003.
- [2] J.-P. Jolivet, E. Tronc, C. Chanéac, Iron oxides: From molecular clusters to solid. A nice example of chemical versatility, *C. R. Geosciences* 338 (2006), 488-497.
- [3] V. Mathé, F. Lévêque, Trace magnetic minerals to detect redox boundaries and drainage effects in a marshland soil in western France, *Eur. J. Soil Science* 56 (2005), 737-751.
- [4] W. Feitknecht, G. Keller, Über die Dunkelgrünen Hydroxyverbindungen des Eisens, *Z. Anorg. Allg. Chem.* 262 (1950), 61-68.
- [5] J.D. Bernal, D.R. Dasgupta, A.L. Mackay, The oxides and hydroxides of iron and their structural inter-relationships, *Clay Miner. Bull.* 4 (1959), 15-30.
- [6] J. Detournay, M. Ghodsi, R. Derie, Etude cinétique de la formation de goethite par aération de gels d'hydroxyde ferreux, *Ind. Chim. Belg.* 39 (1974), 695-701.
- [7] J. Detournay, R. Derie, M. Ghodsi, The region of stability of GR II in the electrochemical potential-pH diagram of iron in sulphate medium, *Corros. Sci.* 15 (1975), 295-306.
- [8] J. Detournay, R. Derie, M. Ghodsi, Etude de l'oxydation par aération de $\text{Fe}(\text{OH})_2$, *Z. Anorg. Allg. Chem.* 427 (1976), 265-273.
- [9] J.-M. R Génin, D. Rézel, Ph. Bauer, A.A. Olowe, A Beral, Mössbauer spectroscopy characterization and electrochemical study of the kinetics of oxidation of iron in chlorinated aqueous media: structure and equilibrium diagram of green rust one, *Materials Sci. Forum* 8 (1986), 477-490.
- [10] A.A. Olowe, J.M.R. Génin, The mechanism of oxidation of Fe(II) hydroxide in sulphated aqueous media : importance of the initial ratio of the reactants, *Corros. Sci.* 32 (1991), 965-984.
- [11] A. A. Olowe, B. Pauron, J.-M. R. Génin, The influence of temperature on the oxidation

of ferrous hydroxide in sulphated aqueous medium: activation energies of formation of the products and hyperfine structure of magnetite, *Corros. Sci.* 32 (1991), 985-1001.

[12] Ph. Refait, J.-M.R. Génin, The oxidation of Fe(II) hydroxide in chloride-containing aqueous media and Pourbaix diagrams of green rust I, *Corros. Sci.* 34 (1993), 797-819.

[13] Ph. Refait, J.B. Memet, C. Bon, R. Sabot, J.-M.R. Génin, Formation of the Fe(II)-Fe(III) hydroxysulphate green rust during marine corrosion of steel, *Corros. Sci.* 45 (2003), 833-845.

[14] Ph. Refait, A. Charton, J. -M.R. Génin, Identification, composition, thermodynamic and structural properties of a pyroaurite-like iron(II)-iron(III) hydroxy-oxalate green rust, *Europ. J. Sol. State Inorg. Chem.* 35 (1998), 655-666.

[15] A. A. Olowe, P. Refait, J.-M.R. Génin, Influence of concentration on the oxidation of ferrous hydroxide in basic sulphated aqueous medium : particle size analysis of goethite and delta FeOOH, *Corros. Sci.* 32 (1991), 1003-1020.

[16] A. A. Olowe, J.-M. R. Génin, The influence of concentration on the oxidation of ferrous hydroxide in acidic sulphated aqueous medium: particle size analysis of lepidocrocite, *Corros. Sci.* 32 (1991), 1021-1028.

[17] Ph. Refait, O. Benali, M. Abdelmoula, J.-M.R. Génin, Formation of 'ferric green rust' and/or ferrihydrite by fast oxidation of iron(II-III) hydroxychloride green rust, *Corros. Sci.* 45 (2003), 2435-2449.

[18] P. Rochette, P.-E. Mathé, L. Esteban, H. Rakoto, J.-L. Bouchez, Q. Liu, J. Torrent, Non-saturation of the defect moment of goethite and fine-grained hematite up to 57 Teslas, *Geophys. Res. Lett.* 32 (2005), 1-4.

[19] R. Thompson, F. Oldfield, "Environmental magnetism", Allen and Unwin, London, 1986, p. 227.

[20] J. Walden, F. Oldfield, J.P. Smith, "Environmental magnetism : A practical guide", Technical guide n°6, Quaternary Research Association, London, 1999, p. 243.

- [21] B. A. Maher, Magnetic properties of some synthetic sub-micron magnetites, *J. Roy. Astr. Soc.* 94 (1988), 83-96.
- [22] W. Lowrie, Identification of ferromagnetic minerals in a rock by coercivity and unblocking temperature properties, *Geophys. Res. Lett.* 17 (1990), 159-162.
- [23] C. Chanéac, E. Tronc, J. P. Jolivet, Magnetic iron oxide-silica nanocomposites. Synthesis and characterization, *J. Mater. Chem.* 6 (1996), 1905-1911.
- [24] P. Cambier, Infrared study of goethites of varying crystallinity and particle size: I. Interpretation of OH and lattice vibration frequencies, *Clay Minerals* 21 (1986), 191-200.
- [25] D. G. Lewis, V. C. Farmer, Infrared absorption of surface hydroxyl groups and lattice vibrations in lepidocrocite (γ -FeOOH) and boehmite (γ -AlOOH), *Clay Minerals* 21 (1986), 93-100.
- [26] G. Lefevre, In situ Fourier-transform infrared spectroscopy studies of inorganic ions adsorption on metal oxides and hydroxides, *Adv. Colloid Interface Sci.* 107 (2004), 109-123.
- [27] Y. Guyodo, A. Mostrom, R. L. Penn, S. K. Banerjee, From Nanodots to Nanorods: Oriented aggregation and magnetic evolution of nanocrystalline goethite, *Geophys. Res. Lett.* 30 (2003), 19-1 – 19-4.
- [28] R. Lee Penn, J. J. Erbs, D. M. Gulliver, Controlled growth of alpha-FeOOH nanorods by exploiting oriented aggregation, *Journal of Crystal Growth* 293 (2006), 1-4.
- [29] O. Ozdemir, D. J. Dunlop, Thermoremanence and Neel temperature of goethite, *Geophys. Res. Lett.* 23 (1996), 921-924.
- [30] P.-E. Mathé, P. Rochette, D. Vandamme, G. Fillion, Néel Temperatures of Synthetic Substituted Goethites and their Rapid Determination Using Low-Field Susceptibility Curves, *Geophys. Res. Lett.* 26 (1999), 2125-2128.
- [31] M. Pernet, X. Obradors, J. Fontcuberta, J.C. Joubert, J. Tejada, Magnetic structure and supermagnetic properties of delta - FeOOH, *IEEE Trans. Magn.* 20 (1984), 1524-1526.

- [32] R. J. Pollard, Q. A. Pankhurst, Ferrimagnetism in fine ferrihydrite particles, *J. Magn. Magn. Materials* 99 (1991), L39-L44.
- [33] M.H. Francombe, H.P. Rooksby, Structure transformations effected by the dehydration of diasporite, goethite and delta ferric oxide, *Clay Min. Bull.* 4 (1959), 1-14.
- [34] T. Ishikawa, W. Yan Cai, K. Kandori, Characterization of the thermal decomposition products of δ -FeOOH by Fourier-transform infrared spectroscopy and N_2 adsorption, *J. Chem. Soc. Faraday Trans.* 88 (1992), 1173-1177.
- [35] A. Manceau, K. L. Nagy, L. Spadini, K. V. Ragnarsdottir, Influence of anionic layer structure of Fe-oxyhydroxides on the structure of Cd surface complexes, *J. Coll. Interf. Sci.* 228 (2000), 306-316.
- [36] G. Patrat, F. De Bergevin, M. Pernet, J.C. Joubert, Structure locale de δ -FeOOH, *Acta Cryst.* B39 (1983), 165-170.
- [37] V.A. Drits, B.A. Sakharov, A. Manceau, Structure of ferrihydrite as determined by simulation of X-ray diffraction curves, *Clay Miner.* 28 (1993), 209-222.

Figure captions

Figure 1: Backfield IRM curves, in $A\ m^2\ kg^{-1}$ and re-scaled to zero, of the final products obtained with the two experimental conditions of reference (I) and (II).

Figure 2: PXRD patterns of the final products obtained with different (a) stirring speeds (rpm) and (b) $FeSO_4$ concentrations ($mol\ L^{-1}$). $R = 2.5$ and $T = 45^\circ C$. hkl are the diffraction lines of goethite with the corresponding Miller index and L(020) is the main diffraction line of lepidocrocite.

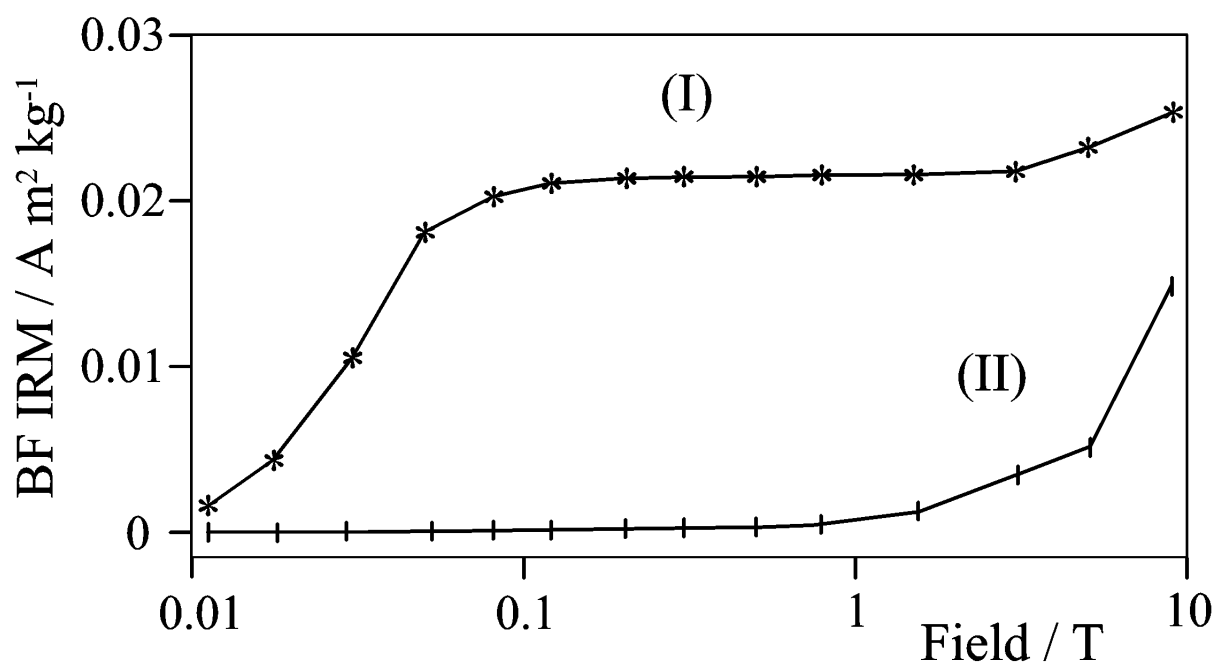
Figure 3: Infrared spectra of the final products obtained with different (a) stirring speeds (rpm) and (b) $FeSO_4$ concentrations ($mol\ L^{-1}$). $R = 2.5$ and $T = 45^\circ C$. The vibration bands of goethite are located at 890, 795 and $630\ cm^{-1}$; those of sulphate ions adsorbed on goethite are denoted as GSO_4^{2-} . Other vibration bands L correspond to lepidocrocite.

Figure 4: (a and b) Backfield IRM curves, in $A\ m^2\ kg^{-1}$ and re-scaled to zero, of the final products obtained with different stirring speeds (rpm) and $FeSO_4$ concentrations ($mol\ L^{-1}$). $R = 2.5$ and $T = 45^\circ C$. (c and d) Magnetic behaviour at low coercivity of the products obtained with (c) $S \geq S_{ref}$ and (d) with the various $FeSO_4$ concentrations considered in the study (Zoom on the 0 – 0.2 T zone of the backfield IRM curves, with magnetic field on x-axis represented in linear scale).

Figure 5: (a and b) TEM images of the final product obtained with $[FeSO_4] = 0.5\ mol\ L^{-1}$ and $S = 760\ rpm$. (c and d) SEM images of the final products obtained respectively with $[FeSO_4] = 1.0\ mol\ L^{-1}$ and $[FeSO_4] = 0.1\ mol\ L^{-1}$. $R = 2.5$ and $T = 45^\circ C$.

Figure 6: Thermal demagnetisation of multi-component IRM. Goethite, prepared with $[FeSO_4] = 0.5\ mol\ L^{-1}$ and $S = 760\ rpm$, was successively magnetised along three orthogonal axes in magnetic fields of 9 T, 3 T and 0.5 T.

Fig 1



Accepted manuscript

Fig 2

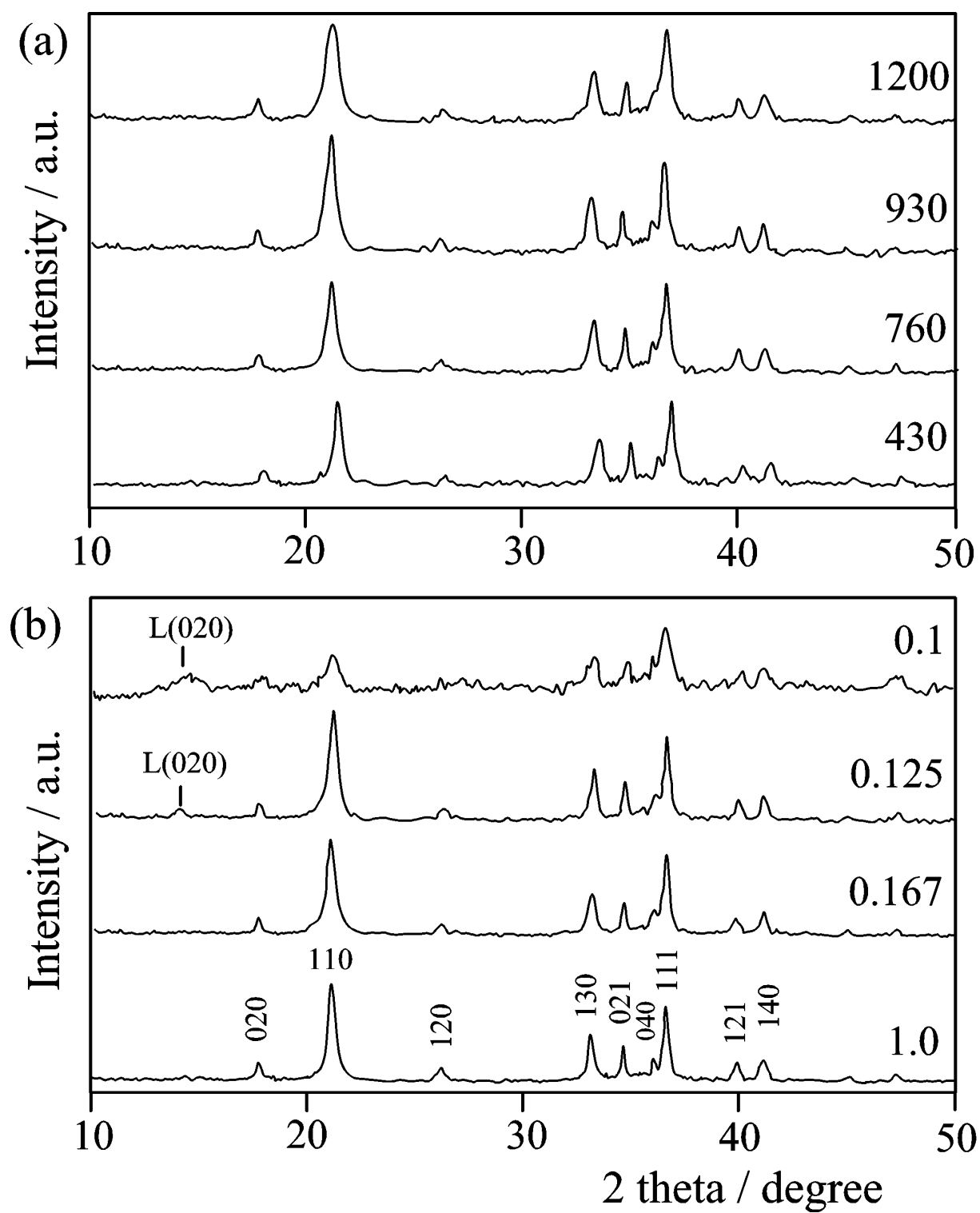


Fig 3

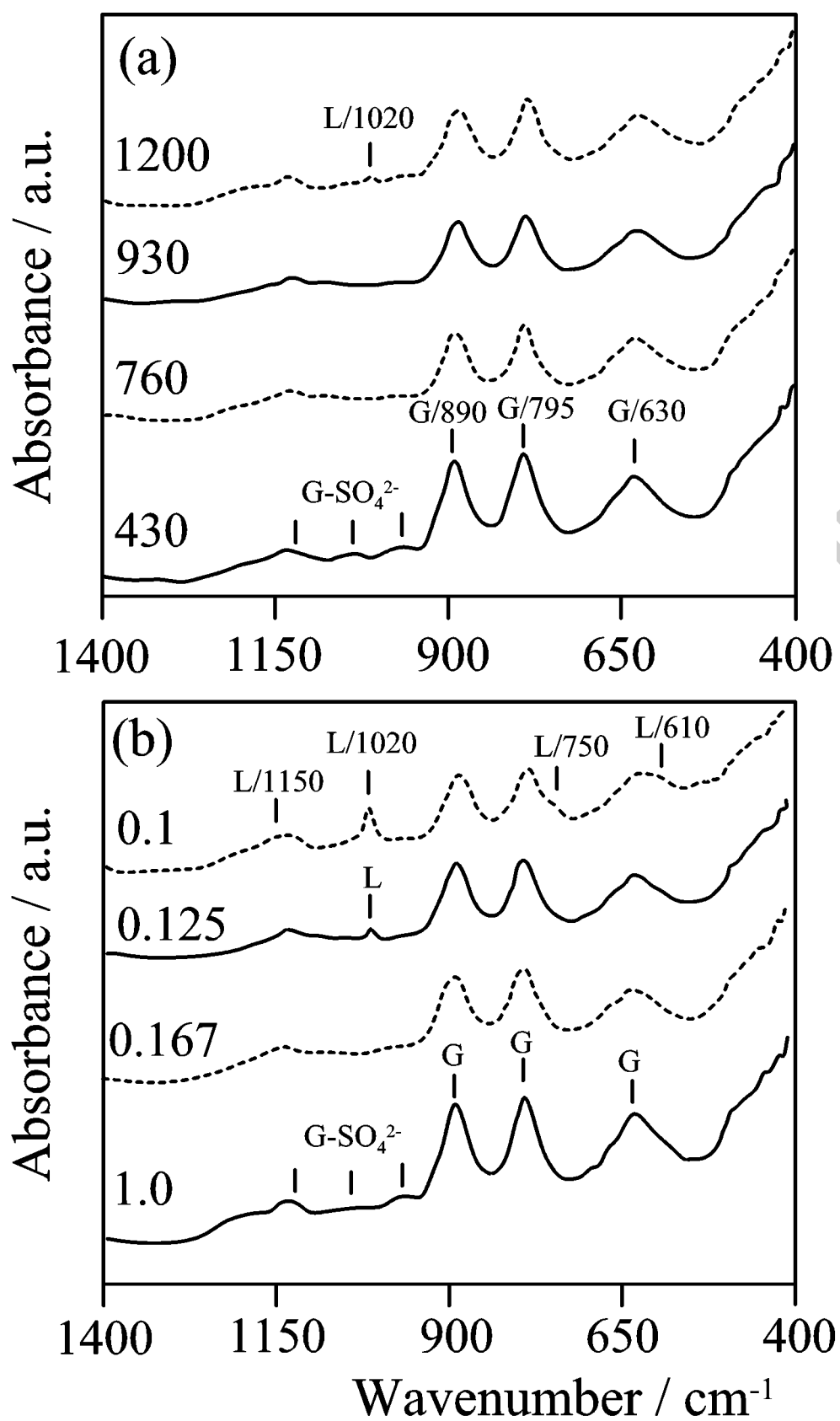


Fig 4

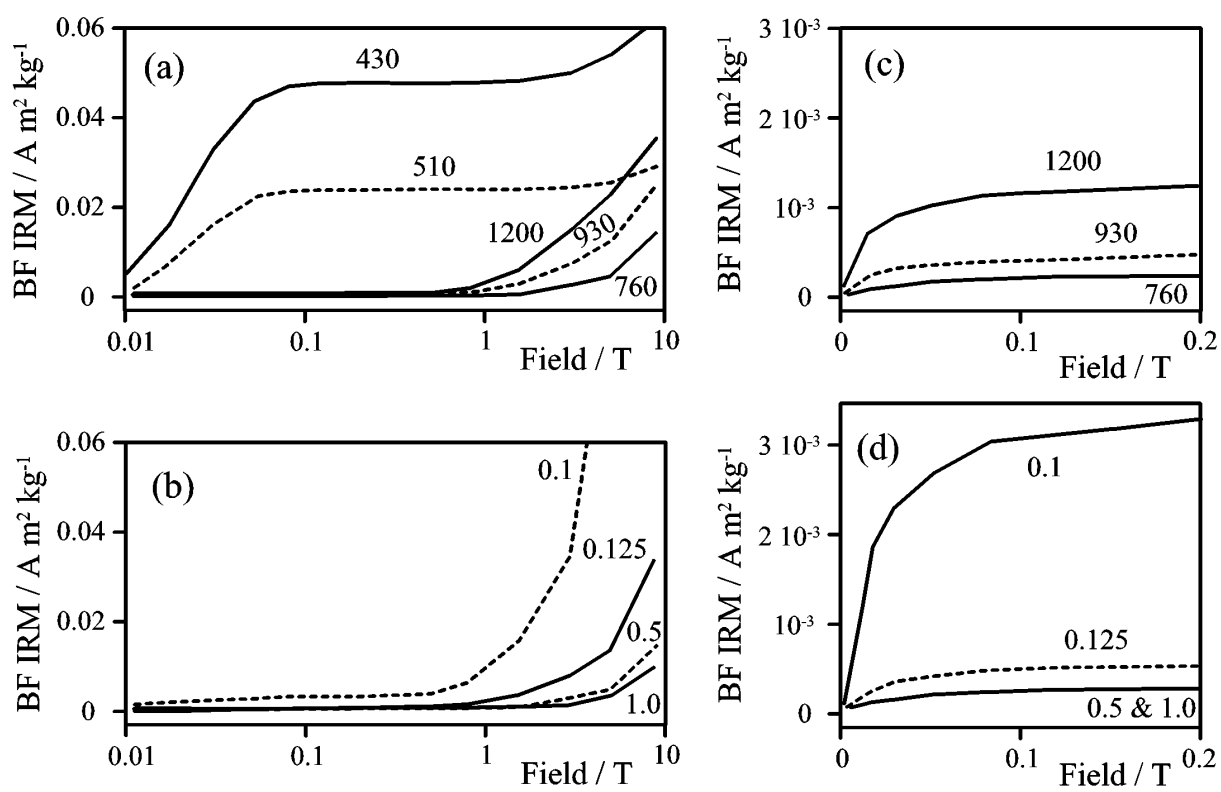
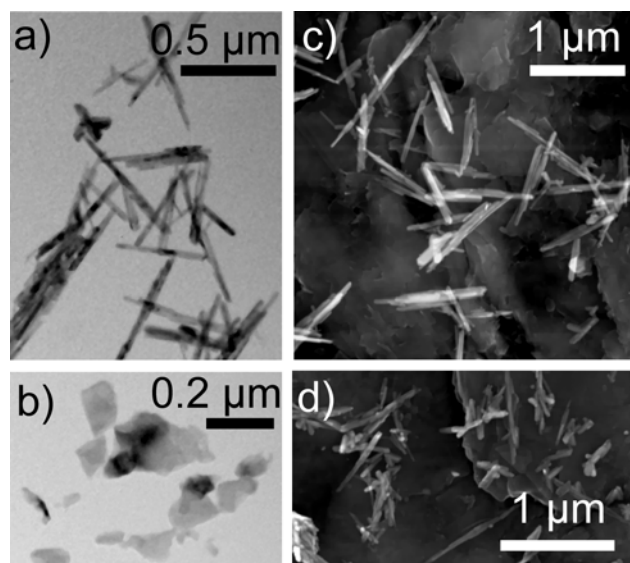
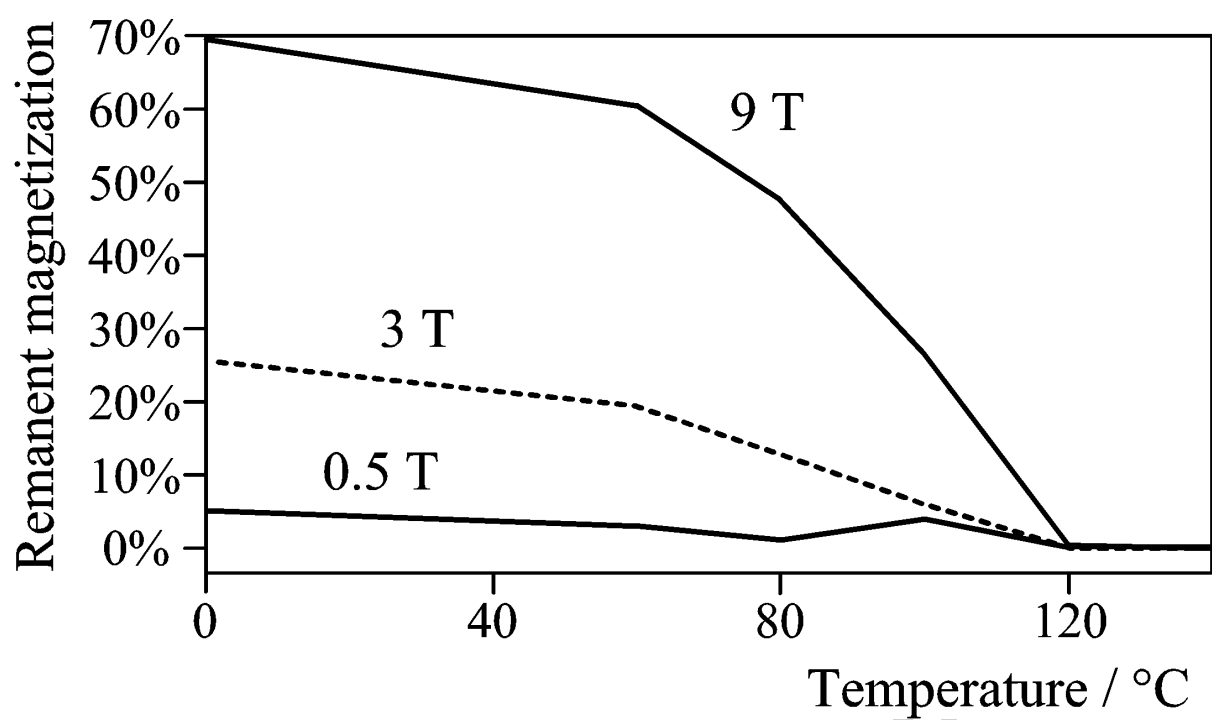


Fig 5



Accepted manuscript

Fig 6



Accepted manuscript